1628 *Inorg. Chem.* **2011**, *50*, 1628–1632
DOI: 10.1021/ic1023086

Inorganic Chemistry
Article

Co_3O_4@graphene Composites as Anode Materials for High-Performance Lithium Ion Batteries

Baojun Li,[†] Huaqiang Cao,*[,†] Jin Shao,[‡] Guoqiang Li,[‡] Meizhen Qu,*[,‡] and Gui Yin[§]

[†]*Department of Chemistry, Tsinghua University, Beijing 100084, People's Republic of China,*
[‡]*Chengdu Institute of Organic Chemistry, Chinese Academy of Sciences, Chengdu 610041, People's Republic of China, and* [§]*Department of Chemistry, Nanjing University, Nanjing 210093, People's Republic of China*

Received September 5, 2010

This paper reports on the synthesis of Co_3O_4@graphene composites (CGC) and their applications as anode materials in lithium ion batteries (LIBs). Through a chemical deposition method, Co_3O_4 nanoparticles (NPs) with sizes in the range of 10−30 nm were homogeneously dispersed onto graphene sheets. Due to their high electrical conductivity, the graphene sheets in the CGC improved the electrical conductivity and the structure stability of CGC. CGC displayed a superior performance in LIBs with a large reversible capacity value of 941 mA hg^{-1} in the initial cycle with a large current density and an excellent cyclic performance of 740 mA hg^{-1} after 60 cycles, corresponding to 88.3% of the theoretical value of CGC, owing to the interactions between graphene sheets and Co_3O_4 NPs anchored on the graphene sheets. This synthesis approach may find its application in the design and synthesis of novel electrode materials used in LIBs.

1. Introduction

In recent years, interest has increased in lithium ion batteries (LIBs) used as green secondary (rechargeable) battery, which can be used repeatedly. The key element of LIBs is that the Li^+ participates in the reactions at both anode and cathode, being reversibly inserted and extracted from the electrode material, accompanying the electron transport. However, it is still a great challenge to find novel electrode and electrolyte materials with improved performance, such as high-energy density and long cycle life as well as high-rate capability. It is required for good electrode materials with high reversible storage capacity for Li in order to reach a long battery life as well as rapid solid-state Li^+ ion and electron transport.[1] Obviously, innovative material chemistry is the key to obtain the various advancements in rechargeable LIBs.[2,3] It has been demonstrated that nanostructured electrode materials are powerful candidates for achieving the quick electrode reaction rates required to deliver high power in rechargeable LIBs.[4−15] Also we know that graphene sheets, being two-dimensional layers of sp^2-hybridized carbon atoms arranged in six-membered rings, have extraordinary electronic transport properties.[16−19] A possible route to obtain the unusual properties may be achieved by incorporating graphene within composite materials. Also Co_3O_4 can theoretically deliver as high as three times the capacity (the theoretical capacity value: ∼890 mA hg^{-1})

*To whom correspondence should be addressed. E-mail: hqcao@mail.tsinghua.edu.cn (H.C.) and mzhqu@cioc.ac.cn (M.Q.).

(1) Kang, K.; Meng, Y. S.; Bréger, J.; Grey, C. P.; Ceder, G. *Science* **2006**, *311*, 977–980.
(2) Croce, F.; Appetecchi, G. B.; Persi, L.; Scrosati, B. *Nature* **1998**, *394*, 456–458.
(3) Kang, B.; Ceder, G. *Nature* **2009**, *458*, 190–193.
(4) Armand, M.; Tarascon, J. M. *Nature* **2008**, *451*, 652–657.
(5) Wagemaker, M.; Kentgens, A. P. M.; Mulder, F. M. *Nature* **2002**, *418*, 397–399.
(6) Nam, K. T.; Kim, D. W.; Yoo, P. J.; Chiang, C. Y.; Meethong, N.; Hammond, P. T.; Chiang, Y. M.; Belcher, A. M. *Science* **2006**, *312*, 885–888.
(7) Derrien, G.; Hassoun, J.; Panero, S.; Scrosati, B. *Adv. Mater.* **2007**, *19*, 2336–2340.
(8) Du, N.; Zhang, H.; Chen, B.; Wu, J.; Ma, X.; Liu, Z.; Zhang, Y.; Yang, D.; Huang, X.; Tu, J. *Adv. Mater.* **2007**, *19*, 4505–4509.
(9) Lou, X. W.; Deng, D.; Lee, J. Y.; Feng, J.; Archer, L. A. *Adv. Mater.* **2008**, *20*, 258–262.
(10) Zhang, W. M.; Hu, J. S.; Guo, Y. G.; Zheng, S. F.; Zhong, L. S.; Song, W. G.; Wan, L. J. *Adv. Mater.* **2008**, *20*, 1160–1165.
(11) Hassoun, J.; Derrien, G.; Panero, S.; Scrosati, B. *Adv. Mater.* **2008**, *20*, 3169–3175.
(12) Yu, Y.; Gu, L.; Wang, C. L.; Dhanabalan, A.; Aken, P. A. V.; Maier, J. *Angew. Chem., Int. Ed.* **2009**, *48*, 6485–6489.
(13) Zhang, H. X.; Feng, C.; Zhai, Y. C.; Jiang, K. L.; Li, Q. Q.; Fan, S. S. *Adv. Mater.* **2009**, *21*, 2299–2304.
(14) Lou, X. W.; Li, C. M.; Archer, L. A. *Adv. Mater.* **2009**, *21*, 2536–2539.
(15) Park, M. H.; Kim, K.; Kim, J.; Cho, J. *Adv. Mater.* **2010**, *22*, 415–418.
(16) Stankovich, S.; Dikin, D. A.; Dommett, G. H. B.; Kohlhaas, K. M.; Zimney, E. J.; Stach, E. A.; Piner, R. D.; Nguyen, S. T.; Ruoff, R. S. *Nature* **2006**, *442*, 282–286.
(17) Novoselov, K. S.; Geim, A. K.; Morozov, S. V.; Jiang, D.; Katsnelson, M. I.; Grigorieva, I. V.; Dubonos, S. V.; Firsov, A. A. *Nature* **2005**, *438*, 197–200.
(18) Zhang, Y.; Tan, Y. W.; Stormer, H. L.; Kim, P. *Nature* **2005**, *438*, 201–204.
(19) Novoselov, K. S.; Geim, A. K.; Morozov, S. V.; Jiang, D.; Zhang, Y.; Dubonos, S. V.; Grigorieva, I. V.; Firsov, A. A. *Science* **2004**, *306*, 666–669.

 Published on Web 01/18/2011

of that of the currently used graphite (~372 mA hg^{-1}), which is expected to meet the requirements of future energy storage systems.[8,9,20] Graphene possesses a large surface area, open porous structure, flexibility, chemical stability, and very high electrical conductivity, which warrants it to be a good candidate for constructing graphene-based composite materials with metal oxides. Some reports on this kind of composite material dealing with preparation methods and applications in rechargeable LIBs with enhanced performances have been reported.[21−28] These achievements inspired us to design novel graphene-based composites and understand their physicochemical behaviors in LIBs. In this paper, we present a simple approach for preparing Co_3O_4@graphene composites (CGC) via a chemical deposition of Co_3O_4 nanoparticles (NPs) onto graphene oxide (GO),[29] followed by reduction of GO to graphene in a $NaBH_4$ solution. The CGC as an anode material in LIBs can afford a high capacity of 940 mA hg^{-1} based on the mass of CGC with good rate capability and cycling stability.

2. Experimental Section

Preparation of CGC. A suspension (200 mL) of GO (0.1 g) was ultrasonicated for 2 h, followed by adding an aqueous solution (10 mL) of $CoCl_2$ (1.4 g $CoCl_2 \cdot 6H_2O$). The mixture was stirred for 2 h to complete the ion exchange. Then, an aqueous solution (10 mL) of NaOH (1 equivalent) was added dropwise into the above mixture with stirring for another 1 h. The solid was obtained via centrifugal method by using deionized water and then dispersed into deionized water (25 mL). Hydroperoxide (30%, 1.5 mL) was added to the above mixture. Ths mixture was sealed into a 50 mL Teflon-lined autoclave, heated to 100 °C, and maintained at this temperature for 4 h. The solid product was collected by using a centrifugal method followed by suspending in deionized water (25 mL). $NaBH_4$ (0.25 g) was added to above suspension, was transferred into autoclave heated to 120 °C, and maintained at this temperature for 4 h. The resulting solid was collected and washed with deionized water and then dried to obtain CGC. Pure Co_3O_4 was obtained via a similar process just in the absence of GO, while graphene was obtained from GO by reduction with $NaBH_4$ via a similar process. For control studies, Co_3O_4@graphite composite material was prepared in a similar process, but graphene was replaced by graphite in the same weight ratio without a reduction process.

Characterization. The morphology of CGC was studied by using transmission electron microscopy (TEM, JEOL JEM-2100, operating at 100 kV) and atom force microscopy (AFM). The samples were coated on a Si surface for AFM studies, and measurements were performed using a Digital Instruments Dimension 3100 microscope in the tapping mode. The Fourier transform infrared (FT-IR) spectra were recorded on a NICOLET 560 FT-IR spectrophotometer. Raman spectra were recorded on a Renishaw RM-1000 with excitation from the 514 nm line of an Ar ion laser with a power of about 5 mW. The phase structures were characterized with X−ray diffraction [XRD, Bruker D8 Advance diffractometer using Cu K_α (λ = 1.5418 Å)]. X−ray photoelectron spectra (XPS) were recorded on a PHI quantera SXM spectrometer with an Al K_α = 280.00 eV excitation source, where binding energies were calibrated by referencing the C1s peak (284.8 eV) to reduce the sample charge effect. The current−voltage ($I-V$) curves were obtained at the CHI660B type electrochemical working station using the compressed pellets (115 mg) of 12.5 mm in diameter, composed of CGC, graphene, and Co_3O_4 samples, respectively, which were processed in a stainless steel mold by using 12 MPa pressure.

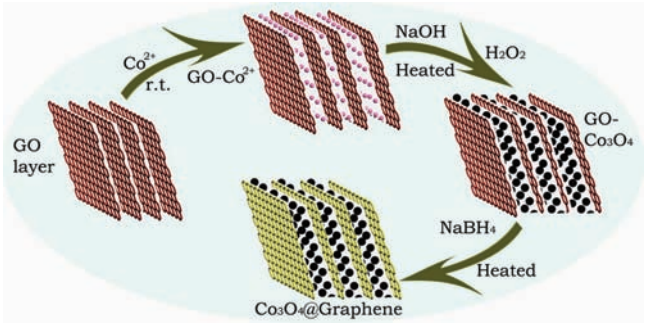

Figure 1. Illustration of the synthesis of CGC from GO.

Electrochemical experiments were performed using CR 2032 type coin cells assembled in an argon-filled glovebox (MBRAUN). The working electrodes prepared by mixing the CGC and carboxymethyl cellulose sodium (CMC, 3 wt.%) at a weight ratio of 90:10 were pasted on pure Cu foil (15 μm). Celgard 2400 was used as a separator. Lithium foil was used as the counter electrode. The electrolyte consisted of a solution of $LiPF_6$ (1 M) containing vinylene carbonate (2 wt.%) in ethylene carbonate/dimethyl carbonate/diethyl carbonate (1:1:1, volume ratio). A galvanostatic cycling test of the assembled cells was carried out on a BS-9300K system in the voltage range of 0.001−3.0 V (vs Li^+/Li) at a current density of 0.2 C (200 mA g^{-1}), 0.5, 1.0, 2.0, and 5.0 C, respectively. The weight of CGC in the working electrode was used to estimate the specific discharge capacity of the battery, which was expressed in mA hg^{-1} of CGC.

3. Results and Discussion

The synthetic process is depicted in Figure 1. The aqueous solution of $CoCl_2$ was added into an aqueous suspension of GO under stirring. After completing ion exchange, an aqueous solution of NaOH (1.0 equivalent) was added dropwise into above mixture. An aqueous solution of H_2O_2 was added into the above mixture with stirring. After hydrothermal treatment, the product was obtained by centrifuge and then heated for drying. The resulted powder was dispersed into deionized water with stirring and ultrasonic treatment, followed by adding $NaBH_4$ into the above disperse system, and then the mixture was heated. Resulting black solid was washed with deionized water, and CGC was obtained.

The morphology of CGC is studied by TEM and AFM. From TEM images, we can find that the sizes of most Co_3O_4 NPs anchored on graphene are in the range of 10−30 nm (Figure 2a and b). A few Co_3O_4 NPs aggregations are observed in TEM images (Figure S1, Supporting Information). The AFM image provides an evidence of the dispersion of Co_3O_4

(20) Wang, X.; Wu, X. L.; Guo, Y. G.; Zhong, Y.; Cao, X.; Ma, Y.; Yao, J. *Adv. Funct. Mater.* **2010**, *20*, 1680–1686.
(21) Paek, S. M.; Yoo, E. J.; Honma, I. *Nano Lett.* **2009**, *9*, 72–75.
(22) Yang, S. B.; Cui, G. L.; Pang, S. P.; Cao, Q.; Kolb, U.; Feng, X. L.; Maier, J.; Mullen, K. *ChemSusChem* **2010**, *3*, 236–239.
(23) Zhang, M.; Lei, D. N.; Yin, X. M.; Chen, L. B.; Li, Q. H.; Wang, Y. G.; Wang, T. H. *J. Mater. Chem.* **2010**, *20*, 5538–5543.
(24) Zhou, G. M.; Wang, D. W.; Li, F.; Zhang, L. L.; Li, N. ; Wu, Z. S.; Wen, L.; Lu, G. Q.; Cheng, H. M. *Chem. Mater.* **2010**, *22*, 5306–5313.
(25) Wang, H. L.; Cui, L. F.; Yang, Y.; Casalongue, H. S.; Robinson, J. T.; Liang, Y. Y.; Cui, Y.; Dai, H. J. *J. Am. Chem. Soc.* **2010**, *132*, 13978–13980.
(26) Guo, C. X.; Yang, H. B.; Sheng, Z. M.; Lu, Z. S.; Song, Q. L.; Li, C. M. *Angew. Chem., Int. Ed.* **2010**, *49*, 3014–3017.
(27) Wu, Z. S.; Ren, W. C.; Wen, L.; Gao, L. B.; Zhao, J. P.; Chen, Z. P.; Zhou, G. M.; Li, F.; Cheng, H. M. *ACS Nano* **2010**, *4*, 3187–3194.
(28) Chen, S. Q.; Wang, Y. *J. Mater. Chem.* **2010**, *20*, 9735–9739.
(29) Hummers, W. S.; Offeman, R. E. *J. Am. Chem. Soc.* **1958**, *80*, 1339–1339.

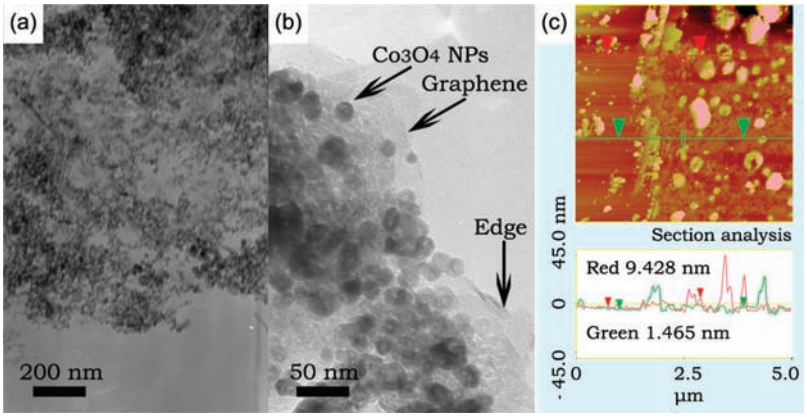

Figure 2. (a, b) Typical TEM images and (c) AFM images of CGC. Inset in (c) is a cross-section analysis of CGC.

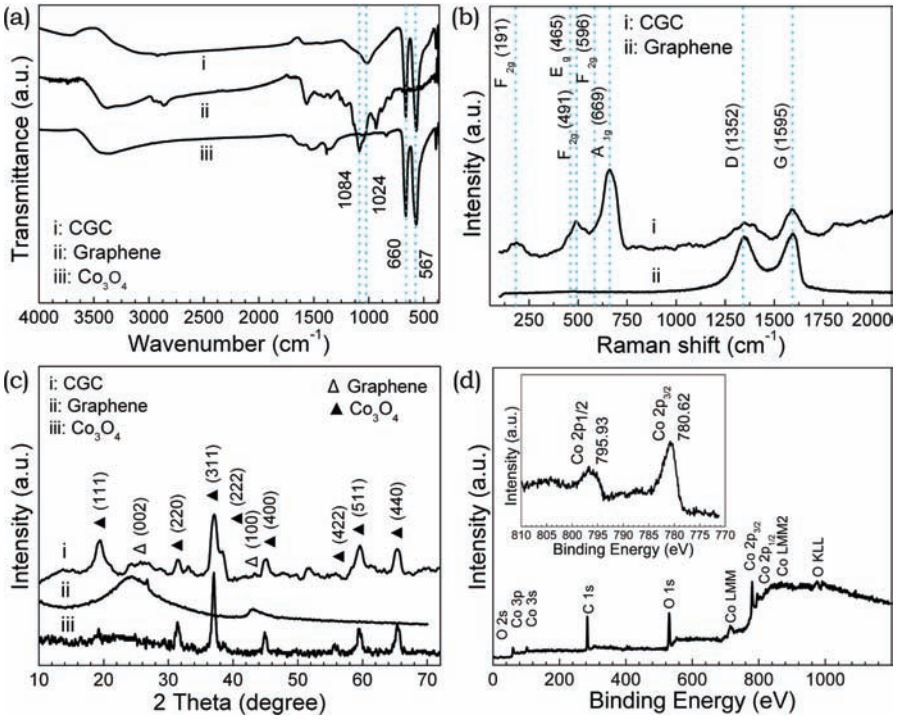

Figure 3. (a) FT-IR spectra of CGC, graphene, and Co_3O_4, respectively; (b) Raman spectra of the CGC and graphene; (c) XRD patterns of CGC, graphene, and Co_3O_4, respectively; and (d) XPS spectrum of CGC. The inset in (d) is the fine spectrum of Co 2p.

NPs onto graphene sheets (Figure 2c).[30,31] A few large Co_3O_4 NP aggregations can be found in the AFM image, which is consistent with TEM images. The existence of Co_3O_4 NPs on graphene sheets indicates that the binding of Co_3O_4 NPs to graphene is unaffected after reduction process. The cross-section analysis indicates a height of ~1.5 nm for the graphene and a height of 10−50 nm for Co_3O_4, respectively. On the basis of graphene sheet thickness, the graphene in CGC may be mono- or bilayer, which is consist with the faint shape in TEM images.[19,30]

In FT-IR spectra of CGC (Figure 3a), the absorption band at 597 and 660 cm^{-1} can be assigned to the vibrations of the Co−O. The absorption at 1564 cm^{-1} can be assigned to the stretching vibration of C═C.[32,33] In the Raman spectra of CGC and graphene (Figure 3b), the G band (~1595 cm^{-1}) corresponding to sp^2-hybridized carbon, and the D band (~1352 cm^{-1}) originating from disordered carbon is observed for both of the samples.[34] The peaks of Raman shift at 191, 491, and 596 cm^{-1} can be attributed to the F_{2g} mode of Co_3O_4, and the peaks at 465 and 669 cm^{-1} can be attributed to the E_g and A_{1g} modes of Co_3O_4, respectively. These results demonstrate the existence of both graphene and Co_3O_4 in the as−prepared composites.

(30) Li, X. L.; Zhang, G. Y.; Bai, X. D.; Sun, X. M.; Wang, X. R.; Wang, E. G.; Dai, H. J. *Nat. Nanotechnol.* **2008**, *3*, 538–542.
(31) Li, D.; Müller, M. B.; Gilje, S.; Kaner, R. B.; Wallace, G. G. *Nat. Nanotechnol.* **2008**, *3*, 101–105.
(32) Dong, Z.; Fu, Y. Y.; Han, Q.; Xu, Y. Y.; Zhang, H. *J. Phys. Chem. C* **2007**, *111*, 18475–18478.
(33) Wang, G. X.; Yang, J.; Park, J.; Gou, X. L.; Wang, B.; Liu, H.; Yao, J. *J. Phys. Chem. C* **2008**, *112*, 8192–8195.
(34) Ferrari, A. C.; Meyer, J. C.; Scardaci, V.; Casiraghi, C.; Lazzeri, M.; Mauri, F.; Piscanec, S.; Jiang, D.; Novoselov, K. S.; Roth, S.; Geim, A. K. *Phys. Rev. Lett.* **2006**, *97*, 187401.

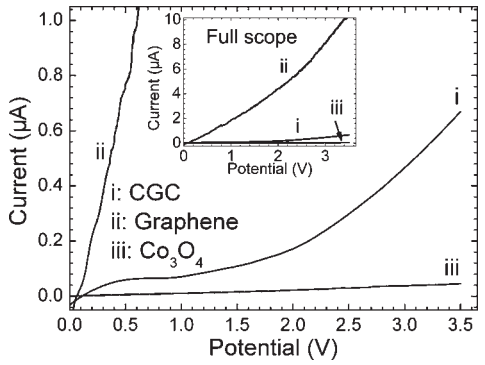

Figure 4. The $I-V$ curves of CGC, graphene, and Co_3O_4, respectively.

In XRD patterns of CGC, graphene, and Co_3O_4 (Figure 3c), the positions and relative intensities of diffraction peaks match well with standard Co_3O_4 and graphene patterns. The peaks at 2θ values of 19.3° (111), 31.5° (220), 37.0° (311), 38.5° (222), 45.0° (400), 55.9° (422), 59.6° (511), 65.4° (440), and 70.2° (531) are consistent with the standard XRD data for the cubic phase Co_3O_4 (JCPDS no. 42-1467). The additive peaks at 24.3° (002) and 43.6° (100) can be attributed to the graphene.[35] In the XPS spectrum of CGC (Figure 3d), the peaks located at 780.62 and 795.93 eV are assigned to the binding energy of Co $2p_{3/2}$ and Co $2p_{1/2}$, respectively. The XPS spectrum reveals that the Co_3O_4 is obtained after reduction.[21,36] The peak at 284.6 eV is assigned to the characteristic peaks of C 1s. The peak at 286.2 eV can be attributed generally to surface-adsorbed hydrocarbons and their oxidative forms (e.g., C−OH and epoxide).[37] The predominant O 1s peak at 531.54 and 532.41 eV belongs to the lattice oxygen combined with Co^{2+} and Co^{3+} in Co_3O_4.

Graphene sheets are good conductors in comparison to Co_3O_4 NPs, which can function as a conductive network or a current collector for Co_3O_4 NPs. As a total matrix, CGC should have better conductivity than that of Co_3O_4 NPs themselves. The current−voltage curves of CGC, graphene, and Co_3O_4 show that CGC provides a significantly higher current than that of Co_3O_4 in the potential range of 0−3.5 V (a potential range for LIBs), which means that CGC possesses an enhanced charge conductivity compared to Co_3O_4 NPs (Figure 4). This higher conductivity indicates the somewhat enhanced performances of LIBs should be obtained for CGC.[38,39]

A standard method based on a CGC−Li half cell was used to evaluate the electrochemical behavior. Figure 5a shows different cycle discharge−charge voltage profiles for CGC at a current density of 200 mA g^{-1}. The theoretical capacity (C) of the hypothetical mixture of CGC is calculated as follows:[31,40]

$$C_{\text{theoretical}} = C_{Co_3O_4} \times \text{mass percentage of } Co_3O_4 + C_{\text{graphite}} \times \text{mass percentage of graphite} = 890 \times 90\% + 372 \times 10\% = 838\text{mA hg}^{-1}$$

The first discharge specific capacity of CGC is about 1276 mA hg^{-1}, which is much larger than the theoretical prediction value for CGC. This phenomenon is attributed to the formation of a solid electrolyte interphase (SEI) layer generated by an irreversible insertion/deinsertion of Li ions into host structures or on Li alloying reactions (eq 1−3) and by possible interfacial Li storage.[8,40,41] Similar phenomena have been observed for metal oxide anodes.[8,9,20] The first discharge exhibits a well-defined long voltage plateau at ca. 0.94−1.0 V associated with the two-phase intercalation process between CGC and $Li_xCo_3O_4$, followed by a sloping curve down to ca. 1.0 mV, which is a typical characteristic of voltage trends for Co_3O_4 electrode.[20,27] After cycling, the load curves show continuous variation of potential. Electrode reactions in rechargeable LIBs rely on simultaneous intercalation of Li^+ and e^- into the active intercalation host of a composite electrode. Hence, the process involves the generation and reduction of Li_2O, accompanying with the reduction and oxidation of metal Co NPs. The final product consists of a homogeneous distribution of Co NPs embedded in a Li_2O matrix. The process indicates that nanoscale materials can change the reaction pathway, which leads to the high capacities and excellent cyclic performances.

$$\text{CGC} + 8\text{Li}^+ + 8\text{e}^- \leftrightarrow 3\text{Co@graphene} + 4\text{Li}_2\text{O} \quad (1)$$

$$8\text{Li} \leftrightarrow 8\text{Li}^+ + 8\text{e}^- \quad (2)$$

$$\text{CGC} + 8\text{Li} \leftrightarrow 4\text{Li}_2\text{O} + 3\text{Co@graphene} \quad (3)$$

Figure 5b shows the typical results of the cycling and stability testing of Li/CGC cells, with cycle−life performance of the CGC up to 60 cycles at a rate of 0.2 C. The specific capacity in the second discharge cycle is 941 mA hg^{-1}. There is no significant capacity loss from the first discharge cycle. The capacity after 60 cycles remains at 740 mA hg^{-1}, corresponding to 83.1% of the theoretical prediction value of Co_3O_4, which is close to the results at a low current density of 50 mA g^{-1} (0.05 C, corresponding to the full discharge in 20 h) in literature.[9,27] This result indicates that the CGC materials present the excellent rate capability performance. At a higher current density (current rates of 0.5−5.0 C), some higher discharge capacities than those of Co_3O_4@graphite are obtained for CGC (Figure 5c). After charging−discharging at a high current rate, the high capacities remained for CGC. A control experiment was carried out with Co_3O_4@graphite composites as anode materials in LIBs at a rate of 0.2 C, which provided a much lower discharge capacity than CGC

(35) Petitto, S. C.; Marsh, E. M.; Carson, G. A.; Langell, M. A. *J. Mol. Catal. A: Chem.* **2008**, *281*, 49–58.
(36) Fan, X. B.; Peng, W. C.; Li, Y.; Li, X. Y.; Wang, S. L.; Zhang, G. L.; Zhang, F. G. *Adv. Mater.* **2008**, *20*, 4490–4493.
(37) Ren, Y.; Armstrong, A. R.; Jiao, F.; Bruce, P. G. *J. Am. Chem. Soc.* **2010**, *132*, 996–1004.
(38) Zhan, F. M.; Geng, B. Y.; Guo, Y. J. *Chem.—Eur. J.* **2009**, *15*, 6169–6174.
(39) *Green Rechargeable Batteries and New System Research Process*; Wu, F., Ed.; Science Publisher: Beijing, China, 2007.
(40) Poizot, P.; Larunelle, S.; Grugeon, S.; Tarascon, M. *J. Electrochem. Soc.* **2002**, *149*, A1212–A1217.
(41) Martha, S. K.; Grinblat, J.; Haik, O.; Zinigrad, E.; Drezen, T.; Miners, J. H.; Exnar, I.; Kay, A.; Markovsky, B.; Aurbach, D. *Angew. Chem., Int. Ed.* **2009**, *48*, 8559–8563.

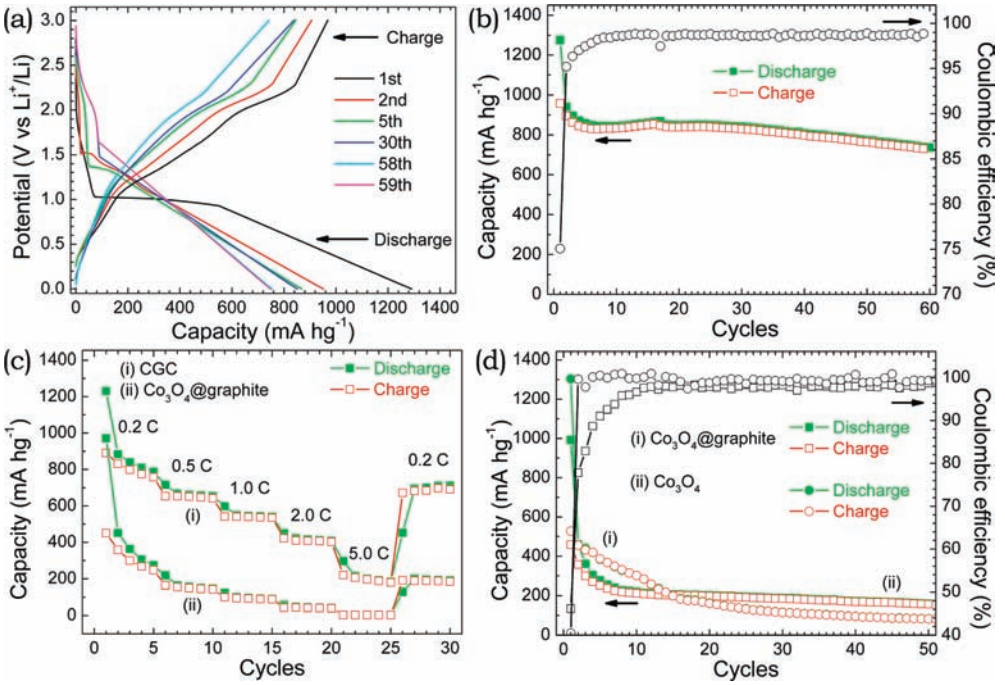

Figure 5. (a) Charge−discharge curves of CGC, (b) cyclic performances of electrodes fabricated by CGC at current rate of 0.2 C (1 C = 1000 mA g^{-1}, corresponding to the full discharge in 5 h, a rate of n C corresponds to the full discharge in $1/n$ h), (c) the charge−discharge performances of CGC and Co_3O_4@graphite at various current rates, and (d) cyclic performances of electrodes fabricated by Co_3O_4@graphite and Co_3O_4 at a current rate of 0.2 C. The weight of CGC in the working electrode was used to estimate the specific discharge capacity of the battery.

(Figure 5d). This means the capacity retention of the CGC is superior due to the layer structure of graphene.

The excellent performance of CGC in LIBs can be attributed to the highly stable layer−structure of graphene. Nanostructured CGC favors the Li^+ ion and the electron transport in LIBs, due to the extraordinary electronic transport property and high surface area of graphene, which is a highly conductive matrix and support for anchoring Co_3O_4 NPs. Due to the close contact between graphene and Co_3O_4 NPs, graphene can serve as an impediment against the deleterious reactions between active matter and solution species in charging−discharging processes.[24] The graphene sheets made Co_3O_4 NPs highly dispersive in CGC and prevent their agglomeration, and then layered structure CGC cannot be destroyed after Li^+ transport.[21,25] Co_3O_4 NPs coated with layered graphene sheets can shorten the diffusion path for ions and electrons.[4,24,25] For serviceable LIBs, the stable and tightened voltage window is an important factor influencing the performances of whole batteries. The voltage windows of LIBs depend on the anode materials, whose voltage window can be evaluated by the corresponding half cell. In the present case, the CGC−Li half cell provided a 0−3.0 V voltage window, which included a 3.0−1.5 step with quickly decreased voltage. This means that a whole battery with CGC will need a low-charging voltage in the primitive stage of the charging process and provides a low-discharging voltage in the last stage of discharging process. Considering that a multistep reaction is involved in LIBs with metal oxide as the anode material, the tightened voltage window is still one of the big challenges of metal oxide anodes in LIBs.[25,27,28] Further study is needed for this favorable aim.

4. Conclusions

In conclusion, a simple and scalable preparation approach of nanostructured CGC was developed via a chemical reduction process of GO in a $NaBH_4$ solution. The cycle performance was determined for up to 60 cycles with an excellent cycle stability and high-rate capability. CGC demonstrated enhanced Li^+ ion intercalation properties for not only superior electronic conductivity but also layer−structure of graphene and possessed a specific discharge capacity of 941 mA hg^{-1} in the initial cycle and 740 mA hg^{-1} after 60 cycles (corresponding to 88.3% of theoretical prediction value of CGC). These superior performances of CGC in LIBs are due to their high surface area and excellent conductivity of graphene sheets as well as short Li^+ ion diffusion paths. From these results, it can be concluded that CGC is a very promising material for use as an anode of LIBs.

Acknowledgment. Financial support from the National Natural Science Foundation of China (no. 20921001 and 20535020), the Innovation Method Fund of China (no. 20081885189), the National High Technology Research and Development Program of China (no. 2009AA03Z321), the Jiangsu Province Foundation of Natural Science (no. BK2006717), and the China Postdoctoral Science Foundation (no. 20100470302) is acknowledged.

Supporting Information Available: Experimental details for preparation of GO and the magnified TEM images of CGC. This material is available free of charge via the Internet at http://pubs.acs.org.